Jpn. J. Cancer Res. **92**, 343–351, March 2001

Antitumor Activity and Pharmacokinetics of TAS-106, 1-(3-*C*-Ethynyl-β-D-*ribo*-pentofuranosyl)cytosine

Yuji Shimamoto,[1] Akio Fujioka,[1] Hiromi Kazuno,[1] Yuko Murakami,[1] Hideyuki Ohshimo,[1] Toshiyuki Kato,[1] Akira Matsuda,[2] Takuma Sasaki[3] and Masakazu Fukushima[1, 4]

[1]The Second Cancer Research Laboratory, Taiho Pharmaceutical Co., Ltd., 1-27 Misugidai, Hanno 357-8527, [2]Graduate School of Pharmaceutical Sciences, Hokkaido University, Kita-12 Nishi-6, Kita-ku, Sapporo 060-0812 and [3]Cancer Research Institute, Kanazawa University, 13-1 Takara-machi, Kanazawa 920-0934

We examined the effects of dosage schedule on antitumor activity *in vitro* and *in vivo* to determine the optimal administration schedule for a new nucleoside antimetabolite 1-(3-*C*-ethynyl-β-D-*ribo*-pentofuranosyl)cytosine (ECyd, TAS-106). The cytotoxicity of TAS-106 *in vitro* against human tumors was evaluated at three drug exposure periods. TAS-106 exhibited fairly potent cytotoxicity even with 4 h exposure, and nearly equivalent and sufficiently potent cytotoxicity with 24 and 72 h exposures. These results suggest that long-term exposure to TAS-106 will not be required to achieve maximal cytotoxicity. The antitumor activity of TAS-106 *in vivo* was compared in nude rat models bearing human tumors on three administration schedules, once weekly, 3 times weekly, and 5 times weekly for 2 or 4 consecutive weeks. TAS-106 showed strong antitumor activity without serious toxicity on all three schedules, but the antitumor activity showed no obvious schedule-dependency in these models. When tumor-bearing nude rats were given a single i.v. dose of [^{3}H]TAS-106, tumor tissue radioactivity tended to remain high for longer periods of time as compared to the radioactivity in various normal tissues. Furthermore, when the metabolism of TAS-106 in the tumor was examined, it was found that TAS-106 nucleotides (including the active metabolite, the triphosphate of TAS-106) were retained at high concentrations for prolonged periods. These pharmacodynamic features of TAS-106 may explain the strong antitumor activity without serious toxicity, observed on intermittent administration schedules, in nude rat models with human tumors. We therefore consider TAS-106 to be a promising compound which merits further investigation in patients with solid tumors.

Key words: 1-(3-*C*-Ethynyl-β-D-*ribo*-pentofuranosyl)cytosine — TAS-106 — TAS-106 nucleotides — Antitumor activity — Pharmacokinetics

Nucleoside antimetabolites are among the most important agents for cancer chemotherapy. We and others have recently demonstrated that 2′-deoxycytidine analogues, such as 1-(2-deoxy-2-methylene-β-D-*erythro*-pentofuranosyl)cytosine (DMDC),[1, 2] 2′-deoxy-2′,2′-difluorocytidine (Gemcitabine),[3, 4] 1-(2-*C*-cyano-2-deoxy-β-D-*arabino*-pentofuranosyl)cytosine (CNDAC),[5–7] and (*E*)-2′-deoxy-2′-(fluoromethylene)cytidine (MDL 101 731),[8, 9] have potent antitumor activities against a wide variety of solid tumors both *in vitro* and *in vivo*. The antitumor activity of these 2′-deoxycytidine analogues is believed to be due mainly to their inhibiting DNA synthesis in tumor cells. However, many solid tumor cells grow slowly, and a drug has little chance of encountering the S phase, in which DNA synthesis occurs. Thus, a chemotherapeutic agent which affects mechanisms other than DNA synthesis would be of benefit.

1-(3-*C*-Ethynyl-β-D-*ribo*-pentofuranosyl)cytosine (TAS-106) is a new analogue of cytidine (Fig. 1) which has shown good preclinical antitumor activity against solid tumors of human origin.[10, 11] The main mechanism of action of TAS-106 is inhibition of RNA synthesis. Pulses with radioactive precursors of macromolecules indicated that incubation of cells with TAS-106 preferentially inhibits its RNA synthesis relative to the synthesis of DNA and protein.[11–13] Studies with an *in vitro* model system of RNA polymerase II indicated that the triphosphate of TAS-106, ECTP, inhibited the enzyme in a concentration-dependent manner.[14] Moreover, the action of TAS-106 on RNA polymerase-specific transcription was demonstrated to be without specificity for RNA polymerase I, II or III in whole K562 human leukemia cells.[12] Thus, TAS-106 inhibits RNA synthesis by blocking RNA polymerases. Co-incubation with cytidine (or uridine) and TAS-106 blocked the cytotoxic activity of the analogue.[11] This suggests competition for transport into the cell and/or for phosphorylation. Cells that are deficient in uridine/cytidine kinase (UCK, EC 2.7.1.48) are actually resistant to TAS-106.[14] When cells were treated with TAS-106 for

[4] To whom correspondence should be addressed.
E-mail: fukusima@taiho.co.jp

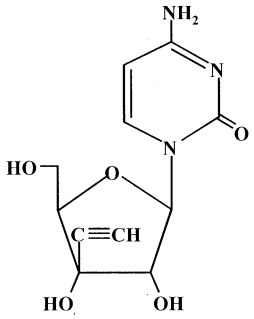

Fig. 1. Chemical structure of TAS-106.

more than 4 h, ECTP accumulated as the major intracellular metabolite and was very slowly eliminated from the cells.[12, 13] Therefore, initial phosphorylation by UCK is apparently necessary for the cytotoxicity of TAS-106, and accumulation and retention of the active metabolite ECTP probably contribute to the potent cytotoxicity of TAS-106. These unique profiles make TAS-106 a promising therapeutic agent for human solid tumors.

In the present study, to determine the optimal administration schedule for TAS-106, we examined the effects of dosage schedule on antitumor activity in various human solid tumors *in vitro* and *in vivo*. In addition, to assess the correlation between the antitumor activity and the pharmacokinetics of TAS-106, we investigated the distribution of radioactivity in tissues and drug metabolism in the tumor following the administration of a single i.v. dose of [^{3}H]TAS-106 to nude rats with human tumor xenografts.

MATERIALS AND METHODS

Chemicals TAS-106 was synthesized by Taiho Pharmaceutical Co., Ltd. (Tokyo). [Cytosine-5(*n*)-^{3}H]TAS-106 (5.4 Ci/mmol, 37 MBq/ml) was synthesized by Amersham International (Buckinghamshire, UK). TAS-106 was dissolved in distilled water for *in vitro* studies or in saline for *in vivo* studies. [^{3}H]TAS-106 solution was prepared by adding the radioactive TAS-106 to non-radioactive TAS-106 dissolved in saline.

Cytotoxic studies *in vitro* A549 human lung, MIAPaCa-2 human pancreas and MCF-7 human breast tumor cells were purchased from Dainippon Pharmaceutical Co., Ltd. (Osaka). NUGC-3 human stomach and HT-29 human colon tumor cells were supplied by Dr. Makoto Inaba of the Cancer Chemotherapy Center, Japanese Foundation for Cancer Research (Tokyo). A549 cells were maintained in Dulbecco's modified Eagle's medium supplemented with 10% heat-inactivated fetal calf serum (FCS; Intergen, Purchase, NY) at 37°C and 5% CO_2. MCF-7 cells were cultured in Eagle's minimum essential medium with non-essential amino acids, supplemented with 1 m*M* sodium pyruvate and 10% FCS. NUGC-3 and HT-29 cells were cultured in RPMI1640 medium supplemented with 10% FCS. MIAPaCa-2 cells were maintained in Dulbecco's modified Eagle's medium supplemented with 10% FCS and 2.5% horse serum (ICN Biomedicals, Inc., Aurora, OH). Cells in the exponential growth phase were seeded onto 6-well plates (5×10^4 cells/1.8 ml/well) on day 0. Twenty-four hours after seeding, on day 1, TAS-106 (6 concentrations ranged from 0 to 100 μM) was added to cultured cells (3 wells at each concentration) at a volume of 0.2 ml/well. On the other hand, to determine the number of cells at the start of drug treatment, cells in each well of one plate (6 wells) were harvested and the cells were counted with an F-300 microcell counter (Sysmex, Kobe). After 4 and 24 h, on the 4 and 24 h TAS-106 exposure schedules, the drug-containing medium was removed, and the cells were washed twice with Dulbecco's phosphate-buffered saline and subsequently cultured in drug-free medium until day 4. On the 72 h exposure schedule, after adding the drug, cells were cultured continuously until day 4. On day 4, cell numbers were determined and converted to values related to the cell numbers on day 1. Relative cell growth was expressed by the formula (mean cell number on day 4)/(mean cell number on day 1)−1. The concentration of TAS-106 which inhibited cell growth by 50% (IC_{50}) was calculated from this relative cell growth. Two or three individual experiments were conducted on each cell line to confirm reproducibility.

Evaluation of antitumor activity *in vivo* OCUM-2MD3 human stomach tumor was supplied by Dr. Yong-Suk Chun, Osaka City University Medical School (Osaka), and LX-1 human lung tumor was provided by Dr. Makoto Inaba of the Cancer Chemotherapy Center, Japanese Foundation for Cancer Research (Tokyo). SC-2 human stomach, PAN-4 human pancreas, and LC-11 and Lu-61 human lung tumors were obtained from the Central Institute for Experimental Animals (Kawasaki). A human tumor grown s.c. in nude mice was cut into approximately 2 mm cubes and transplanted s.c. into male F344/N Jcl-rnu nude rats (CLEA Japan, Inc., Tokyo). When tumor volume reached 200−500 mm^3, the animals were assigned randomly to control or drug treatment groups of 8 animals each (day 0), and received drugs via the caudal vein at a volume of 1 ml/100 g body weight starting the next day (day 1). Mean tumor volume was 245.8 mm^3 (SD±32.4 mm^3) and mean body weight of nude rats was 283.3 g (SD±22.0 g) on day 0 in this study (all of 6 experiments). To assess antitumor effects, tumor volumes were measured twice weekly and changes were monitored. Tumor volume was calculated using the formula $L\times W^2/2$, where L is the length (longest diameter) and W is the width (shortest diameter) of the tumor, and the tumor volumes were converted to values related to the initial tumor volume. This relative tumor

volume was expressed by the formula V_n/V_0, where V_n is the volume on any given day and V_0 is the volume on day 0. In addition, the tumor growth inhibition rate (IR, %) was calculated from the ratio of the mean relative tumor volume of treated tumors to that of control tumors (T/C) according to the formula $(1-T/C)\times 100\%$ at 2 or 4 weeks after the initial injection (day 15 or 29).

Measurement of tissue distribution and metabolism in tumors Nude rats s.c. transplanted with LX-1 human lung tumors were given a single i.v. dose of [^{3}H]TAS-106 (6 mg/kg, 3.7 MBq/kg). For analysis of the distribution of radioactivity and intratumoral drug metabolism, serum and various tissues (tumor, skin, lung, liver, kidney, spleen, small intestine, large intestine, testis, brain, and bone marrow cells) were sampled from 3 rats at each of the following 6 time points: 0.5, 1, 2, 4, 8 and 24 h after i.v. administration. At each point in time, bone marrow cells were collected from the 3 rats and combined into a cell pellet. All samples of serum, bone marrow cell pellets, and tissues were immediately frozen on dry ice and stored at −30°C until used.

Radioactivity due to [^{3}H]TAS-106 was measured in each tissue by combustion and oxidation of each tissue sample and then collecting the tritium in the form of tritiated water. Each tissue sample was cut into 0.5 g pieces. Each piece was carefully weighed and placed in a Combust Cone to dry spontaneously. The Combust Cone containing the dry tissue sample was then placed in a Model 307 automated sample oxidizer (Packard Japan, Inc., Tokyo) for combustion and oxidation. Tritiated water released as a product of combustion and oxidation was collected, combined with 12 ml of Monophase-S scintillator (Packard), and the radioactivity was measured with an LSC-5100 liquid scintillation counter (Aloka, Tokyo). To measure the radioactivity of serum samples, 0.5 ml of serum was placed in a Combust Cone into which a Combust Pad had been placed. To measure the radioactivity of bone marrow cells, the cell pellet was weighed and combined with saline, and then treated ultrasonically. Finally, 0.5 ml of the homogenate (total 2 ml) was placed in a Combust Cone with a Combust Pad.

Drug metabolism in the tumor was assessed by the following procedure. Each tumor sample was cut into 0.5 g pieces. Then, each piece was carefully weighed, combined with 2 ml of ice-cold 4% perchloric acid (PCA), and homogenized with a "Polytron" homogenizer. The homogenate was centrifuged, and the supernatant (the acid-soluble fraction) and the pellet (the acid-insoluble fraction) were separated. The acid-soluble fraction was neutralized with KOH, and then centrifuged to remove the precipitate. The entire supernatant was evaporated to dryness, and the residue was dissolved in 100 μl of distilled water. A 20 μl sample of this concentrated acid-soluble fraction was spotted onto a silica gel 60 F_{254} thin-layer chromatography plate (2.5×10 cm, Merck KGaA, Darmstadt, Germany) and developed with a mixed solution of chloroform/methanol/acetic acid (14/6/1, v/v/v), and TAS-106 nucleotides left behind at the origin and the developed TAS-106 were separated. Each fraction was scraped off and placed in a vial, 0.5 ml of 1 *N* HCl and 10 ml of ACS-II scintillator (Amersham) were added, and the radioactivity was measured. On the other hand, the acid-insoluble fraction, which contained RNA and DNA, was washed twice with 4% PCA. The pellet was suspended in 1 ml of distilled water, combined with 4 ml of ethanol, and then centrifuged. The pellet obtained was suspended in 4 ml of a mixed solution of ethanol/diethyl ether (1/1, v/v), heated at 37°C for 10 min, and centrifuged. A 2 ml volume of 0.3 *N* KOH was added to this pellet, and the RNA was alkali-hydrolyzed at 37°C for 16–20 h. After cooling, the specimen was neutralized with PCA, and the final PCA concentration was subsequently raised to 4%. The precipitate was removed by centrifugation, and the supernatant obtained was used as the RNA fraction. The pellet, on the other hand, was washed with 4% PCA, resuspended in 2 ml of 4% PCA, heated in a boiling water bath for 15 min, and the DNA was acid and thermally decomposed. After cooling, the specimen was centrifuged, and the supernatant obtained was used as the DNA fraction. The entire sample of each RNA and DNA fraction was placed in a separate vial, 18 ml of ACS-II was added, and the radioactivity in all vials was measured.

RESULTS

Effect of drug exposure time on cytotoxicity The cytotoxicity of TAS-106 *in vitro* against five human solid tumors of lung (A549), stomach (NUGC-3), colon (HT-29), pancreas (MIAPaCa-2), and breast (MCF-7) origin, at three different drug exposure periods of 4, 24 and 72 h, was evaluated. The results are summarized in Table I. The IC_{50} values of TAS-106 in the five human tumors with 4, 24 and 72 h exposure ranged from 0.114 to 1.032 μM, 0.015 to 0.067 μM, and 0.008 to 0.058 μM, respectively.

Table I. Effect of Drug Exposure Time on the Cytotoxicity of TAS-106 in Five Human Tumor Cell Lines

Drug exposure time (h)	IC_{50} [a)] value (μM)				
	A549 (Lung)	NUGC-3 (Stomach)	HT-29 (Colon)	MIAPaCa-2 (Pancreas)	MCF-7 (Breast)
4	0.114	1.032	0.539	0.198	0.326
24	0.020	0.054	0.067	0.015	0.030
72	0.008	0.025	0.058	0.009	0.015

a) IC_{50}, 50% inhibitory concentration; values are from single representative experiments performed in triplicate.

These results suggest that the cytotoxicity of TAS-106 tends to become stronger as the exposure time becomes longer. However, the differences in IC_{50} values between the 24 and 72 h exposure times were not large, and TAS-106 appeared to show sufficiently potent cytotoxicity at the 24 h exposure time in all 5 human tumors. Even at the 4 h exposure time, TAS-106 clearly showed potent cytotoxicity with IC_{50} values at submicromolar concentrations in 4 of the 5 human tumors. When the area under the concentration×time curve (AUC, IC_{50}×exposure time) values were calculated, AUC at 4 h for NUGC-3 cell line (4.13 $\mu M \cdot$h) and that at 72 h for HT-29 cell line (4.18 $\mu M \cdot$h) were remarkably higher than the others. However, the AUC values are almost constant on each cell line if these two values are omitted.

Schedule dependency of *in vivo* antitumor activity In the first step of the *in vivo* experiment, equitoxic and minimum toxic doses of TAS-106 on three different schedules, once weekly (administered on day 1 and day 8), 3 times weekly (on days 1, 3, 5, 8, 10 and 12), and 5 times weekly (on days 1–5 and days 8–12) for 2 consecutive weeks, were assessed in non-tumor-bearing nude rats. At these doses, the rats were required to lose no more than 10% of their initial weight at 2 weeks after the first i.v. injection (day 15). Five doses were administered on each schedule. On the once weekly schedule, doses of 6 and 12 mg/kg led to a mean weight loss of 4.2% (SD±2.4%) and 22.7% (SD±4.9%) on day 15, respectively, and all 8 animals died due to toxicity at 24 mg/kg. On the 3 times weekly schedule, doses of 1 and 2 mg/kg led to a mean weight loss of 2.9% (SD±2.6%) and 14.9% (SD±7.6%), respectively, and death due to toxicity occurred in 7 of the 8 animals at

Table II. Antitumor Activity of the Equitoxic and Minimum Toxic Doses of TAS-106 on Various Administration Schedules in Nude Rat Models with Human Tumor Xenografts

Tumor (Origin)	Dose of TAS-106 (mg/kg)	Administration schedule	Toxicity Weight loss (Mean±SD, %)[a]		Antitumor effect IR (%)[b]	
			Day 15	Day 29	Day 15	Day 29
		2 consecutive weeks				
OCUM-2MD3	6	Once weekly[c]	5.2±4.7	—	91.8	—
(Stomach)	1	3 times weekly[d]	5.4±1.3	—	89.2	—
	0.3	5 times weekly[e]	2.0±2.2	—	90.8	—
LX-1	6	Once weekly	6.7±3.8	—	98.0	—
(Lung)	1	3 times weekly	6.9±2.8	—	90.6	—
	0.6	5 times weekly	8.3±1.7	—	94.8	—
Lu-61	6	Once weekly	8.9±1.9	—	56.3	—
(Lung)	1	3 times weekly	8.4±3.6	—	83.0	—
	0.4	5 times weekly	9.4±2.6	—	85.1	—
		4 consecutive weeks				
SC-2	6	Once weekly[f]	5.1±3.4	3.5±3.3	76.9	94.7
(Stomach)	1	3 times weekly[g]	3.7±2.3	4.9±4.6	74.7	92.4
PAN-4	6	Once weekly	2.9±2.3	5.4±2.6	89.1	97.2
(Pancreas)	1	3 times weekly	2.5±2.0	8.2±4.4	89.2	95.8 [1/8][h]
LC-11	6	Once weekly	3.8±1.7	8.7±3.7	99.1 [5/8]	99.9 [6/8]
(Lung)	1	3 times weekly	3.5±2.8	8.8±2.8	90.5	96.4 [1/8]

a) Weight loss on day 15 or 29 was expressed as a percentage of the initial weight on day 0; values, mean of eight rats±SD.
b) IR, tumor growth inhibition rate: calculated from relative tumor volume; see "Materials and Methods."
c) Once weekly for 2 consecutive weeks: administered on days 1 and 8.
d) Three times weekly for 2 consecutive weeks: administered on days 1, 3, 5, 8, 10 and 12.
e) Five times weekly for 2 consecutive weeks: administered on days 1–5 and 8–12.
f) Once weekly for 4 consecutive weeks: administered on days 1, 8, 15 and 22.
g) Three times weekly for 4 consecutive weeks: administered on days 1, 3, 5, 8, 10, 12, 15, 17, 19, 22, 24 and 26.
h) Numbers in square brackets, tumor-free rats.

4 mg/kg. On the 5 times weekly schedule, doses of 0.3 and 0.6 mg/kg led to a mean weight loss of 2.7% (SD±1.8%) and 9.7% (SD±4.5%), respectively, and death due to toxicity occurred in 6 of the 8 animals at 1.2 mg/kg. Therefore, 6 mg/kg once weekly, 1 mg/kg 3 times weekly, and 0.3 mg/kg 5 times weekly were considered to be equitoxic and minimum toxic doses of TAS-106 in non-tumor-bearing nude rats. These equitoxic doses were adjusted in tumor-bearing rats, as required.

Next, the equitoxic doses of TAS-106 on three different schedules were simultaneously injected i.v. into nude rats with human tumors for 2 consecutive weeks to determine the appropriate administration schedule (Table II and Fig. 2). Three human tumors were used: OCUM-2MD3 stomach, LX-1 lung and Lu-61 lung. While the dose of TAS-106 on the 5 times weekly schedule was adjusted in each tumor model, administration of TAS-106 at doses of 6 mg/kg once weekly, 1 mg/kg 3 times weekly, and 0.3–0.6 mg/kg 5 times weekly led to nearly the same weight loss in nude rats regardless of the tumor type. In both OCUM-2MD3 and LX-1 xenografts, tumor regression was noted and a very potent antitumor effect with an IR on day 15 of approximately 90% or even higher was observed at the minimum toxic doses of TAS-106 on all three administration schedules. In particular, administration of TAS-106 at 6 mg/kg once weekly exhibited a marked tumor shrinking effect with an IR of 98% against the LX-1 tumor. The Lu-61 tumor was not as sensitive as the OCUM-2MD3 and LX-1 tumors, and no remarkable tumor regression occurred. While TAS-106 treatment on an either 3 or 5 times weekly schedule had a potent antitumor effect with an IR of approximately 85%, the IR of TAS-106 once weekly was less than 60% and its antitumor effect was rather weak. Next, the antitumor effects of TAS-106 at 6 mg/kg once weekly (administered on days 1, 8, 15 and 22) and 1 mg/kg 3 times weekly (on days 1, 3, 5, 8, 10, 12, 15, 17, 19, 22, 24 and 26) for 4 consecutive weeks were compared in nude rat models with SC-2 human stomach, PAN-4 human pancreas, and LC-11 human lung tumors (Table II and Fig. 3). Four consecutive weeks of administration at these TAS-106 doses on both schedules led to nearly the same, mild weight loss of no more than 10% even on day 29 in nude rats regardless of tumor type. In SC-2 and PAN-4 xenografts, tumor regression was noted and a very potent antitumor effect with an IR exceeding 90% was observed on day 29 for both administration schedules. With the LC-11 xenograft, an extremely potent antitumor effect with an IR exceeding 99% was observed on both day 15 and day 29 on the TAS-106 6 mg/kg once weekly schedule. Five of the 8 animals were found to be tumor-free, meaning that the tumor could not be palpated, on day 15, and 6 of the 8 animals were tumor-free on day 29. Although tumor regression was not remarkable, a very potent antitumor effect with an IR

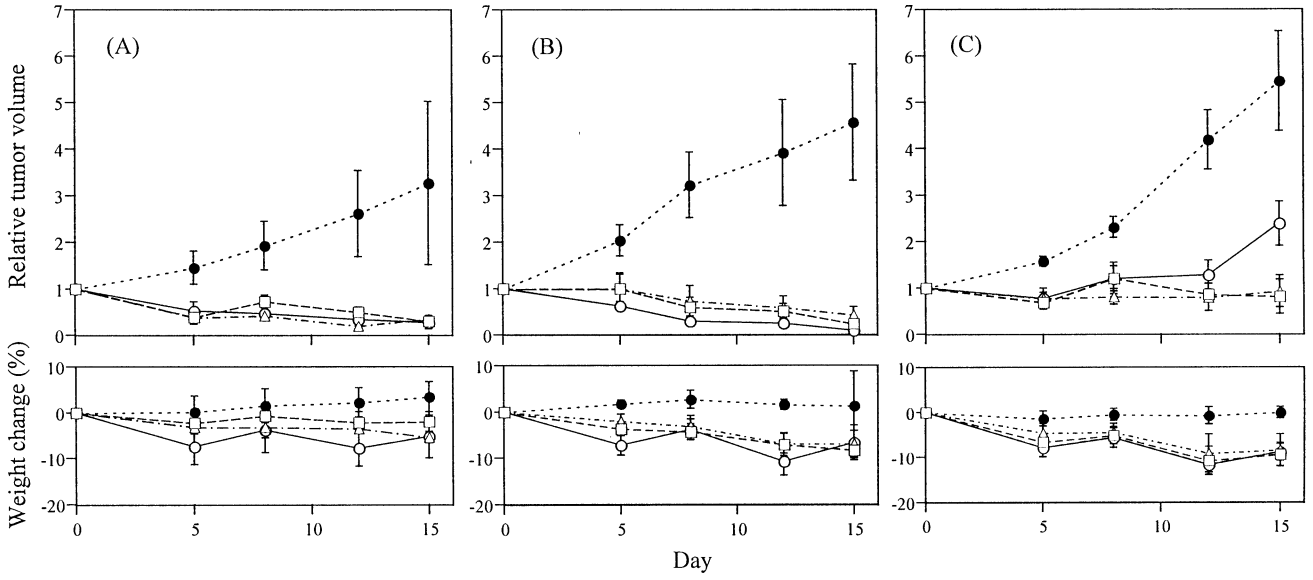

Fig. 2. Antitumor activity of the equitoxic and minimum toxic doses of TAS-106 in nude rat models with three human tumor xenografts: OCUM-2MD3 stomach tumor (A), LX-1 lung tumor (B), and Lu-61 lung tumor (C). TAS-106 was administered on three different schedules for 2 consecutive weeks: control (●); 6 mg/kg once weekly (administered on days 1 and 8) (○); 1 mg/kg 3 times weekly (on days 1, 3, 5, 8, 10 and 12) (△); and 0.3 (A), 0.6 (B) or 0.4 (C) mg/kg 5 times weekly (on days 1–5 and 8–12) (□). Points, mean of eight rats; bars, SD.

exceeding 90% was also observed on both day 15 and day 29 on the TAS-106 1 mg/kg 3 times weekly schedule.

Radioactivity distribution among tissues The radioactivity due to [^{3}H]TAS-106, that is, TAS-106 or its metabolites, was measured in dpm units and then converted into molar concentrations per 1 ml serum or 1 g tissue (Table III). Serum radioactivity was 20.59 nmol/ml 0.5 h after the dose but decreased rapidly thereafter, falling to 0.91

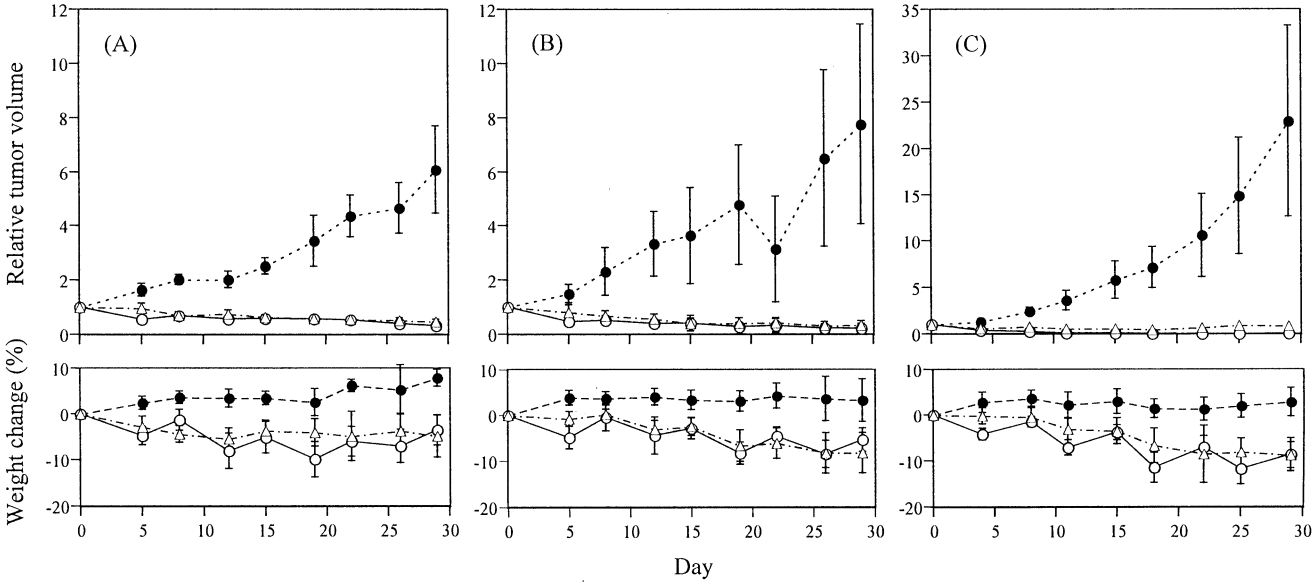

Fig. 3. Antitumor activity of the equitoxic and minimum toxic doses of TAS-106 in nude rat models with three human tumor xenografts: SC-2 stomach tumor (A), PAN-4 pancreatic tumor (B), and LC-11 lung tumor (C). TAS-106 was administered on two different schedules for 4 consecutive weeks: control (●); 6 mg/kg once weekly (administered on days 1, 8, 15 and 22) (○); 1 mg/kg 3 times weekly (on days 1, 3, 5, 8, 10, 12, 15, 17, 19, 22, 24 and 26) (△). Points, mean of eight rats; bars, SD.

Table III. Tissue Distribution of TAS-106 and Its Metabolites in Nude Rats with LX-1 Human Lung Tumors

Tissue	Distribution of TAS-106 and its metabolites (nmol/ml serum or g tissue)[a]						AUC[c] (nmol·h/ml or g)
	0.5 h	1 h	2 h	4 h	8 h	24 h	
Serum	20.59±2.57	7.48±0.98	4.03±0.18	2.14±0.29	0.91±0.01	0.22±0.02	39.23
Tumor	24.42±3.49	25.32±1.69	24.80±1.32	29.19±1.72	25.08±0.43	16.01±3.59	534.85
Kidney	74.80±31.88	24.79±2.35	18.78±3.64	8.23±1.50	3.12±0.29	0.54±0.08	144.37
Liver	27.28±4.18	16.01±1.77	11.72±0.33	10.02±1.46	5.81±0.29	0.87±0.03	138.35
Small intestine	17.78±5.83	14.83±1.12	12.62±0.67	10.42±2.82	5.87±0.25	0.79±0.10	135.22
Spleen	16.55±1.97	12.42±0.40	10.10±0.60	7.79±1.80	3.81±0.36	0.78±0.03	100.45
Lung	18.04±1.56	11.70±1.58	9.20±0.37	6.70±0.58	3.66±0.40	0.69±0.03	93.82
Large intestine	16.26±1.02	11.68±2.68	7.38±2.92	6.44±1.07	2.95±0.38	0.69±0.21	82.30
Bone marrow[b]	8.52	3.70	7.68	8.09	2.11	0.19	65.45
Skin	16.41±1.76	7.75±1.00	5.56±0.49	3.93±0.43	2.16±0.16	0.80±0.16	62.15
Testis	7.20±1.05	4.88±0.52	4.02±0.86	3.30±0.43	2.15±0.14	0.68±0.09	50.13
Brain	0.86±0.32	0.52±0.04	0.44±0.07	0.44±0.04	0.39±0.02	0.28±0.02	8.94

Nude rats s.c. transplanted with LX-1 human lung tumors were given a single i.v. does of [^{3}H]TAS-106 (6 mg/kg, 3.7 MBq/kg), and serum, tumor, and other tissues were sampled from three rats at each of the indicated time points. Radioactivity due to [^{3}H]TAS-106 in each tissue was measured by combustion and oxidation, and then collecting the tritium in the form of tritiated water; see "Materials and Methods."

a) Radioactivity due to [^{3}H]TAS-106 was measured in dpm units and then converted into molar concentrations per 1 ml serum or 1 g tissue; values, mean of three rats±SD.

b) Bone marrow cells, at each point in time, were collected from the three rats and combined into a cell pellet.

c) AUC, area under the concentration×time curve; calculated from the radioactivity levels between 0.5 and 24 h.

nmol/ml at 8 h and 0.22 nmol/ml at 24 h. The AUC for the radioactivity levels between 0.5 and 24 h after the dose was 39.23 nmol·h/ml. Tumor tissue radioactivity ranged between approximately 24 and 29 nmol/g during the period from 0.5 to 8 h after the dose and remained at 16.01 nmol/g even at 24 h. The AUC for tumor tissue radioactivity from 0.5 to 24 h after the dose was 534.85 nmol·h/g, and more than 13 times higher than the serum radioactivity. The AUCs for radioactivity in the other normal tissues were in the following order: kidney>liver> small intestine > spleen > lung > large intestine > bone marrow cells > skin > testis> brain. Thus, radioactivity was much lower in the brain than in other normal tissues. The radioactivity level measured 0.5 h after the dose was higher in the kidney than in any other tissue examined. Thereafter, however, renal tissue radioactivity decreased rapidly, as did serum radioactivity. The AUC for renal tissue radioactivity from 0.5 to 24 h after the dose was 144.37 nmol·h/g, and was approximately one-quarter that of tumor tissue. These results suggest that TAS-106 intravenously administered to nude rats is rapidly eliminated by the kidneys via urine. Moreover, when measured 0.5 h after the TAS-106 dose, the radioactivity in normal tissues, other than kidney and brain, was comparable to or lower than tumor tissue radioactivity. Unlike tumor tissue radioactivity, which remained high for long periods of time, radioactivity in these normal tissues decreased at a similar rate after 0.5 h. Radioactivity at 24 h was below 1 nmol/g in all normal tissues, including the kidney and brain.

Tumor tissue metabolism The *in vivo* metabolism of TAS-106 in tumor tissue is illustrated in Fig. 4. The tumor tissue TAS-106 level was 5.11 nmol/g 0.5 h after administration and decreased rapidly thereafter, falling to 0.45 nmol/g (less than 1/10 the level at 0.5 h) at 8 h. The level of TAS-106 nucleotides in tumor tissue tended to remain high for long periods of time, being between approximately 9 and 18 nmol/g from 0.5 to 24 h after the TAS-106 dose, with a T_{max} at 4 h. The radioactivity in RNA tended to be retained for long periods of time, showing a pattern of change similar to that of the tumor level of TAS-106 nucleotides, although the level of radioactivity in RNA was not high. Virtually no radioactivity was incorporated into DNA.

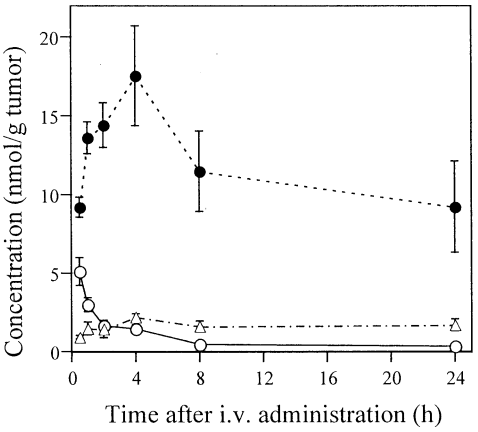

Fig. 4. *In vivo* intratumoral metabolism of TAS-106 after i.v. administration of [^{3}H]TAS-106 (6 mg/kg, 3.7 MBq/kg) into nude rats with LX-1 human lung tumors. The concentrations of TAS-106 (○) and TAS-106 nucleotides (●) in the acid-soluble materials, and the TAS-106 incorporated into RNA (△) of the tumor tissue were measured at the indicated time points as described in "Materials and Methods." Virtually no radioactivity was incorporated into DNA. Points, mean of three rats; bars, SD.

DISCUSSION

TAS-106 is a new and unique *ribo*-nucleoside analogue, which inhibits RNA synthesis by blocking RNA polymerases. TAS-106 reportedly shows potent cytotoxicity against a wide variety of human solid tumor cells on a continuous exposure schedule *in vitro* and strong antitumor activity against various human solid tumor xenografts on a daily administration schedule *in vivo*.[10, 11] In the present study, to determine the optimal administration schedule for TAS-106, we examined the effects of dosage schedule on antitumor activity in various human solid tumors *in vitro* and *in vivo*.

With short-term exposure of tumor cells to TAS-106 *in vitro*, the active metabolite ECTP accumulated rapidly and remained in the cells for long periods of time after the parent TAS-106 had been washed out of the culture medium.[12, 13] In FM3A mouse mammary tumor cells, brief exposure to TAS-106 caused shrinkage of nucleoli and subsequent cell death.[13] In the present *in vitro* experiment using human tumor cells (Table I), although the cytotoxic effect of TAS-106 tended to become stronger as the exposure time became longer, fairly potent cytotoxicity was evident even with 4 h exposure. When the AUC values are calculated, TAS-106 induced cytotoxicity seems to be correlated with AUC. Therefore, we consider that TAS-106 belongs to cell cycle phase-non-specific (AUC-dependent) agents in Inaba's classification.[15, 16] These results suggest that long-term exposure to TAS-106 will not be required to achieve maximal cytotoxicity.

To determine the optimal *in vivo* administration schedule for TAS-106, we compared antitumor activities on the three different schedules, once weekly, 3 times weekly, and 5 times weekly for 2 or 4 consecutive weeks in nude rat models with human stomach (OCUM-2MD3, SC-2), lung (LX-1, Lu-61, LC-11), and pancreatic (PAN-4) tumors (Table II and Figs. 2, 3). The equitoxic and minimum toxic doses of TAS-106 on these administration schedules were different: 6 mg/kg per week on the once weekly schedule, 3 mg/kg per week on the 3 times weekly

schedule, and 1.5–3 mg/kg per week on the 5 times weekly schedule. These doses of TAS-106, however, showed tumor shrinking effects against 5 of the 6 human tumor xenografts with mild weight loss on all of the 2 or 3 schedules tested. Although the antitumor effect of TAS-106 on the once weekly schedule against Lu-61 human lung tumor was rather weak, remarkable tumor regression was observed on the same schedule against the other tumors including LX-1 and LC-11 lung tumors. In general, the antitumor activity of TAS-106 showed no obvious schedule-dependency in these nude rat models, but TAS-106 exhibited excellent antitumor activity even on the intermittent administration schedules.

In this study, we investigated TAS-106 tissue distributions and metabolism in tumor tissue, using nude rats with LX-1 human lung tumors, to assess relationships between the antitumor activities and pharmacokinetics of TAS-106. The distribution of radioactivity due to [^{3}H]TAS-106 was examined (Table III). Serum radioactivity decreased rapidly with time, whereas tumor tissue radioactivity tended to be retained for a longer period of time. The radioactivity in tumor tissue also tended to remain high for longer periods than in normal tissues, such as the digestive tract (small and large intestine), hemopoietic system (spleen and bone marrow), liver, kidney, lung, skin, testis and brain. These results suggest that the distribution of TAS-106 *in vivo* favors tumor tissue. In addition, when the metabolism of TAS-106 in the tumor was examined, it was found that tumor levels of TAS-106 nucleotides tended to remain high for long periods of time while the tumor TAS-106 level decreased rapidly with time (Fig. 4). The nucleoside di- and triphosphates in living tissue are known to be rapidly dephosphorylated to monophosphates during the tissue removal procedure. Therefore, we measured TAS-106 nucleotides collectively in the present study. When tumor cells were exposed to TAS-106 *in vitro*, however, the major metabolite was its triphosphate ECTP, the intracellular concentration of which remained high for long periods of time.[12, 13] We therefore confirmed that ECTP is retained at high concentrations in tumor tissue, as a major metabolite of TAS-106 *in vivo*, as well. The excellent antitumor activity of TAS-106 *in vivo* observed on the intermittent schedules without serious toxicity apparently reflects the pharmacodynamic features of TAS-106, i.e., a tumor-selective distribution of TAS-106 which may be caused by a higher level of phosphorylation and long-term retention of TAS-106 nucleotides in tumor tissue than other normal tissues. Although the level of TAS-106 incorporated into RNA was low, it tended to be retained for a long time, showing a pattern of change similar to that of TAS-106 nucleotides in tumor tissue (Fig. 4). A small amount of ECTP is also reportedly incorporated into RNA as an alternative substrate of RNA polymerase in cells treated with TAS-106.[13, 14] The significance of ECTP incorporation into nucleic acids, with regard to the cytotoxicity of TAS-106, requires further investigation.

The formation of ECTP seems to be crucial for TAS-106 to exert cytotoxic activity. UCK is responsible for the initial phosphorylation of TAS-106.[14] TAS-106 is largely resistant to inactivation via deamination by cytidine deaminase (data not shown). UCK is therefore thought to be a key enzyme in the cellular metabolism of TAS-106 required for this drug to exhibit cytotoxicity. We previously reported UCK activity in human tumor xenografts to be higher than that in various normal tissues of nude rats.[13] The *in vivo* antitumor activity and pharmacokinetics of TAS-106 demonstrated in the present study apparently reflect this characteristic of the enzyme. It is also well known that UCK activity in human cancer tissues is relatively high as compared to that in normal tissues.[17–22] Tumor-selective cytotoxicity of TAS-106 could therefore be expected clinically.

In conclusion, the antitumor activity of TAS-106 showed no obvious schedule-dependency, but this compound did have potent antitumor activity without severe side effects even on intermittent administration schedules in human solid tumor models. This excellent preclinical antitumor efficacy appears to reflect the pharmacodynamic features of TAS-106. We therefore consider TAS-106 to be an interesting compound which merits further investigation in patients with solid tumors.

(Received October 31, 2000/Revised December 14, 2000/ Accepted December 19, 2000)

REFERENCES

1) Takenuki, K., Matsuda, A., Ueda, T., Sasaki, T., Fujii, A. and Yamagami, K. Design, synthesis, and antineoplastic activity of 2′-deoxy-2′-methylidenecytidine. *J. Med. Chem.*, **31**, 1063–1064 (1988).
2) Yamagami, K., Fujii, A., Arita, M., Okumoto, T., Sakata, S., Matsuda, A., Ueda, T. and Sasaki, T. Antitumor activity of 2′-deoxy-2′-methylidenecytidine, a new 2′-deoxycytidine derivative. *Cancer Res.*, **51**, 2319–2323 (1991).
3) Hertel, L. W., Kroin, J. S., Misner, J. W. and Tustin, J. M. Synthesis of 2-deoxy-2,2-difluoro-D-ribose and 2-deoxy-2,2-difluoro-D-ribofuranosyl nucleosides. *J. Org. Chem.*, **53**, 2406–2409 (1988).
4) Hertel, L. W., Boder, G. B., Kroin, J. S., Rinzel, S. M., Poore, G. A., Todd, G. C. and Grindey, G. B. Evaluation of the antitumor activity of Gemcitabine (2′,2′-difluoro-2′-deoxycytidine). *Cancer Res.*, **50**, 4417–4422 (1990).
5) Matsuda, A., Nakajima, Y., Azuma, A., Tanaka, M. and Sasaki, T. Nucleosides and nucleotides. 100. 2′-*C*-Cyano-

2′-deoxy-1-β-D-arabinofuranosylcytosine (CNDAC): design of a potential mechanism-based DNA-strand-breaking antineoplastic nucleoside. *J. Med. Chem.*, **34**, 2917–2919 (1991).

6) Azuma, A., Nakajima, Y., Nishizono, N., Minakawa, N., Suzuki, M., Hanaoka, K., Kobayashi, T., Tanaka, M., Sasaki, T. and Matsuda, A. Nucleosides and nucleotides. 122. 2′-*C*-Cyano-2′-deoxy-1-β-D-arabinofuranosylcytosine and its derivatives. A new class of nucleoside with a broad antitumor spectrum. *J. Med. Chem.*, **36**, 4183–4189 (1993).
7) Tanaka, M., Matsuda, A., Terao, T. and Sasaki, T. Antitumor activity of a novel nucleoside, 2′-C-cyano-2′-deoxy-1-β-D-arabinofuranosylcytosine (CNDAC) against murine and human tumors. *Cancer Lett.*, **64**, 67–74 (1992).
8) McCarthy, J. R., Matthews, D. P., Stemerick, D. M., Huber, E. W., Bey, P., Lippert, B. J., Snyder, R. D. and Sunkara, P. S. Stereospecific method to *E* and *Z* terminal fluoro olefins and its application to the synthesis of 2′-deoxy-2′-fluoromethylene nucleosides as potential inhibitors of ribonucleoside diphosphate reductase. *J. Am. Chem. Soc.*, **113**, 7439–7440 (1991).
9) Bitonti, A. J., Dumont, J. A., Bush, T. L., Cashman, E. A., Cross-Doersen, D. E., Wright, P. S., Matthews, D. P., McCarthy, J. R. and Kaplan, D. A. Regression of human breast tumor xenografts in response to (*E*)-2′-deoxy-2′-(fluoromethylene)cytidine, an inhibitor of ribonucleoside diphosphate reductase. *Cancer Res.*, **54**, 1485–1490 (1994).
10) Hattori, H., Tanaka, M., Fukushima, M., Sasaki, T. and Matsuda, A. Nucleosides and nucleotides. 158. 1-(3-*C*-Ethynyl-β-D-*ribo*-pentofuranosyl)cytosine, 1-(3-*C*-ethynyl-β-D-*ribo*-pentofuranosyl)uracil, and their nucleobase analogues as new potential multifunctional antitumor nucleosides with a broad spectrum of activity. *J. Med. Chem.*, **39**, 5005–5011 (1996).
11) Tabata, S., Tanaka, M., Matsuda, A., Fukushima, M. and Sasaki, T. Antitumor effect of a novel multifunctional antitumor nucleoside, 3′-ethynylcytidine, on human cancers. *Oncol. Rep.*, **3**, 1029–1034 (1996).
12) Azuma, A., Emura, T., Huang, P. and Plunkett, W. Intracellular metabolism and actions of a novel antitumor nucleoside, 1-(3-*C*-ethynyl-β-D-*ribo*-pentofuranosyl)cytosine (ECyd, TAS-106). *Proc. Am. Assoc. Cancer Res.*, **40**, 298 (1999).
13) Takatori, S., Kanda, H., Takenaka, K., Wataya, Y., Matsuda, A., Fukushima, M., Shimamoto, Y., Tanaka, M. and Sasaki, T. Antitumor mechanisms and metabolism of the novel antitumor nucleoside analogues, 1-(3-*C*-ethynyl-β-D-*ribo*-pentofuranosyl)cytosine and 1-(3-*C*-ethynyl-β-D-*ribo*-pentofuranosyl)uracil. *Cancer Chemother. Pharmacol.*, **44**, 97–104 (1999).
14) Tabata, S., Tanaka, M., Endo, Y., Obata, T., Matsuda, A. and Sasaki, T. Anti-tumor mechanisms of 3′-ethynyluridine and 3′-ethynylcytidine as RNA synthesis inhibitors: development and characterization of 3′-ethynyluridine-resistant cells. *Cancer Lett.*, **116**, 225–231 (1997).
15) Ozawa, S., Sugiyama, Y., Mitsuhashi, Y., Kobayashi, T. and Inaba, M. Cell killing action of cell cycle phase-nonspecific antitumor agents is dependent on concentration-time product. *Cancer Chemother. Pharmacol.*, **21**, 185–190 (1988).
16) Ozawa, S., Sugiyama, Y., Mitsuhashi, J. and Inaba, M. Kinetic analysis of cell killing effect induced by cytosine arabinoside and cisplatin in relation to cell cycle phase specificity in human colon cancer and Chinese hamster cells. *Cancer Res.*, **49**, 3823–3828 (1989).
17) Maehara, Y., Nakamura, H., Nakane, Y., Kawai, K., Okamoto, M., Nagayama, S., Shirasaka, T. and Fujii, S. Activities of various enzymes of pyrimidine nucleotide and DNA synthesis in normal and neoplastic human tissues. *Gann*, **73**, 289–298 (1982).
18) Ahmed, N. K., Haggitt, R. C. and Welch, A. D. Enzymes of salvage and *de novo* pathways of synthesis of pyrimidine nucleotides in human colorectal adenocarcinomas. *Biochem. Pharmacol.*, **31**, 2485–2488 (1982).
19) Ahmed, N. K. Enzymes of the *de novo* and salvage pathways for pyrimidine biosynthesis in normal colon, colon carcinoma, and xenografts. *Cancer*, **54**, 1370–1373 (1984).
20) Maehara, Y., Kusumoto, T., Sakaguchi, Y., Kusumoto, H., Kido, Y., Anai, H. and Sugimachi, K. Pyrimidine nucleotide synthesis is more extensive in poorly differentiated than in well-differentiated human gastric carcinoma. *Cancer*, **63**, 96–101 (1989).
21) Maehara, Y., Moriguchi, S., Emi, Y., Watanabe, A., Kohnoe, S., Tsujitani, S. and Sugimachi, K. Comparison of pyrimidine nucleotide synthetic enzymes involved in 5-fluorouracil metabolism between human adenocarcinomas and squamous cell carcinomas. *Cancer*, **66**, 156–161 (1990).
22) Luccioni, C., Beaumatin, J., Bardot, V. and Lefrançois, D. Pyrimidine nucleotide metabolism in human colon carcinomas: comparison of normal tissues, primary tumors and xenografts. *Int. J. Cancer*, **58**, 517–522 (1994).